East European Journal of Physics. **4.** 210-215 (2023)
DOI:10.26565/2312-4334-2023-4-26 ISSN 2312-4334

ELECTRONIC STRUCTURE CALCULATION OF α-Al_2X_3 SYSTEM (X = O, S) BASED ON r++SCAN FUNCTIONAL

Muhammad R. Ramadhan[a], Salwa A. Khansa[a], Q. Zulindra[a], Dian P. Handayani[a], Nina A. Wardani[a], Fahmia Astuti[b]*

[a] *Department of Chemical Engineering, Faculty of Industrial Engineering, UPN Veteran Yogyakarta, 55283 Sleman, Indonesia*
[b] *Department of Physics, Faculty of Science and Data Analytics, Institut Teknologi Sepuluh Nopember, 60111 Surabaya, Indonesia*
**Corresponding Author e-mail: fahmia@physics.its.ac.id*
Received September 25, 2023; revised October 11, 2023; accepted October 31, 2023

Due to the necessity of reducing the reliance on fossil fuels, several systems are considered to be alternative and/or additional support for the existing battery material. In this report, structural and electronic properties of aluminium oxide (Al_2O_3) and aluminium sulfide (Al_2S_3) with hexagonal symmetry (α-phase), are investigated by utilizing density functional theory technique based on r++SCAN functional. The calculated lattice parameter and insulating gap for both systems are well matched with previous experimental studies and display higher accuracy compared to the results from local density approximation (LDA) and generalized gradient approximation (GGA) studies. The calculated insulating gap values are 10.3 eV and 4.1 eV for α-Al_2O_3 and α-Al_2S_3 respectively. For α-Al_2O_3 system, we observed hybridized s-p-d orbital of Al-O in the conduction states, consistent with the interpretation of past X-ray Absorption Near Edge Structure (XANES) data. Finally, the bulk and young modulus for α-Al_2O_3 are determined to be 251 GPa and 423 GPa which is very close to the known experimental values of 280 GPa and 451 GPa.
Keywords: *DFT; meta-GGA; r++SCAN; α-Al_2O_3, α-Al_2S_3*
PACS: 31.15.E−, 31.15.eg, 31.15.es

INTRODUCTION

Recently, global interest is increasing for the development of renewable energy storage material that is clean and affordable, leading to the reduction of reliance on fossil energy. Battery technology based on lithium ion is one of the most researched for the energy storage system. However, due to the current technological advancement, the power density and life cycle of lithium-ion battery does not meet the current global needs [1,2]. This situation motivates many researchers to design an alternative to the lithium-ion battery [3,4]. One such system is the aluminium-based sulfide battery, Al_2S_3, that has been attracted interest recently due to its promising characteristics to achieve low-cost and high-performance energy storage system [5]. It was observed from the experimental studies that Al_2S_3 is stable in $P6_1$ space group symmetry (the so-called α-phase) [6]. On the other aspect, similar α-phase system based on aluminium, Al_2O_3, is also utilized to support the existing lithium-based battery material by coating its surface to improves the electrochemical performance and cycling capacity of the battery [7,8].

Both structure of α-Al_2O_3 and α-Al_2S_3 can be described based on the hexagonal crystal axes, in which both systems contain 12 Al atoms and 18 O or S atoms. For α-Al_2O_3, the lattice parameters of $a = 4.756$ Å and $c = 12.982$ Å is observed at 4.5 K by using Bragg backscattering method [9]. Whereas the lattice parameter for Al_2O_3 is calculated to be $a = 6.438$ Å and $c = 17.898$ Å from a single crystal x-ray diffraction (XRD) refinement [6]. From its electronic properties, both systems are insulating and confirmed experimentally by optical spectroscopy for α-Al_2O_3 [10] and photoconductivity experiment for α-Al_2S_3 [11].

Several theoretical studies have been reported for both of the systems. For α-Al_2O_3 system, it was initially investigated by Xu *et al.,* that an indirect insulating gap of 6.29 eV is obtained from local density approximation (LDA) of density functional theory (DFT) calculation [12]. Following this result, further studies using generalized gradient approximation (GGA) suggested similar insulating gap albeit with direct gap characteristics [13]. Considering that the experimental gap is reported to be 8.8 eV, the calculated values based on LDA and GGA functionals are underestimated [14,15]. Higher gap values can be obtained by employing hybrid functionals such as B3LYP (8.5 eV) and HSE (9.2 eV) [16,17]. For α-Al_2S_3 system, GGA-PBE functional gives a gap value of ~3 eV [18], while hybrid functional of HSE06 gives a higher gap at 4.95 eV [19]. From those theoretical results, the lower gap values from the semilocal functional such as LDA and GGA can be increased by using hybrid functional such as B3LYP and HSE. However, hybrid functional is also known to be very expensive from the perspective of computational resource, making it difficult to utilize this functional on more complex DFT calculation such as surface dynamic and/or atomic substitution effect. Thus, semilocal functional is preferably used for those type of calculation [20], while ignoring the facts that insulating gap is severely underestimated. Based on those facts, more DFT studies with more efficient functional is still required.

Recently, the meta-GGA functional which obeys all 17 known constraints of for the exact exchange-correlation (XC) at semilocal level named SCAN (strongly constrained appropriately normed), attract wide interest due to its accuracy

Cite as: M.R. Ramadhan, S.A. Khansa, Q. Zulindra, D.P. Handayani, N.A. Wardani, F. Astuti, East Eur. J. Phys. 4, 210 (2023), https://doi.org/10.26565/2312-4334-2023-4-26

on predicting different type of materials [21]. Lane *et al.,* report a proper insulating gap values on the Mott-insulator of La_2CuO_4 without any additional parameter [22]. Our group also successfully describe the most realistic structure of superhard material B_4C from the perspective of both electronic and elastic characteristics [23]. Other successful implementation of SCAN is also reported for the problematic germanium atom, in which 0.57 eV gap is opened, contrary to the metallic behavior observed when using GGA-PBE functional [24]. Furthermore, the composite structure made from Si and Ge atom can also be properly described when discussing its composition effects on the calculated gap [25]. However, SCAN functional is also known to suffers numerical instability which leads to the increasing computational cost making it closer to the inefficiency level of hybrid functional [26]. To remedy this, regularized SCAN (rSCAN) functional is developed by Bartok and Yates, which reduces the number of satisfied constraints (13 out of 17 exact constraints) [27]. Further investigation based on rSCAN shows a reduced accuracy compared to the original SCAN functional [28]. To improve this situation, Furness *et al.,* modifies the rSCAN functional and introduces three new functionals with increasing adherence to the constraint named r++SCAN, r^2SCAN, and r^4SCAN [29]. Out of those three new functionals, r^2SCAN is the one that is recommended by the author, to achieve balance between accuracy and numerical performance. Later study by Kingsbury *et al.,* confirm the robustness of r^2SCAN calculation's time with the caveat that the calculated band gap is smaller and larger lattice volumes are obtained for many strongly-bound structures [30]. The fact that r^2SCAN functional predicts larger lattice parameters can also be seen on the original report by Furness *et al.,* where the r^2SCAN has a tendency to overestimate lattice parameters for a system that consists 2 elements such as LiCl, LiF, MgO, NaCl, NaF and SiC. For those type of systems, r++SCAN is actually superior in terms of predicting lattice parameters and achieves the accuracy level of SCAN functional (Furness *et al.,* 2022).

Following those results, we chose r++SCAN functional to investigate the electronic structure of α-Al_2O_3 and α-Al_2S_3 and try to provide more insight on the application of SCAN-type functionals to different type of materials.

COMPUTATIONAL METHODOLOGY

All calculations were conducted based on Quantum Espresso (QE) v.7.0 package [31,32]. The chosen functional for exchange-correlation is r++SCAN which is provided via Libxc v.6.0.0 [33]. The pseudopotential that considers additional kinetic term for the electron density are based on Yao *et al.* [24]. Both α-Al_2O_3 and α-Al_2S_3 are optimized using the kinetic energy cut-off of 80 Rydberg (Ry) to accomodate a denser fast fourier transform (FFT) grids that is necessary for this type of functional. The chosen value for the kinetic energy cut-off is determined by looking into the relation between calculated total energy and its kinetic energy cut-off as depicted in Fig. 1.

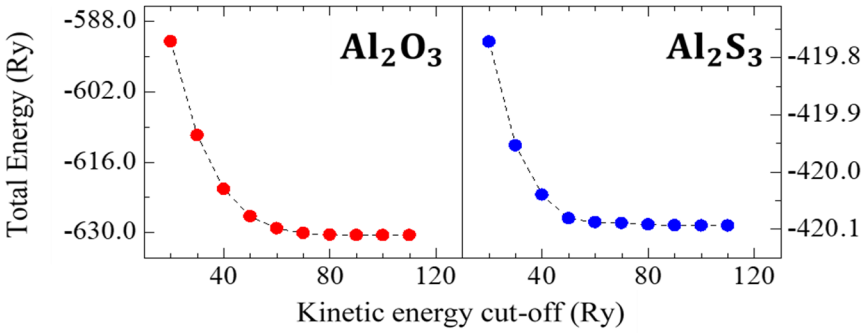

Figure 1. Calculated total energy of Al_2O_3 and Al_2S_3 with respect to kinetic energy cut-off

Brillouin zone of α-Al_2O_3 (α-Al_2S_3) system is considered within the automatic k-points arrangement of $9 \times 9 \times 3$ ($6 \times 6 \times 2$). Then, we expand the k-points to $18 \times 18 \times 6$ ($12 \times 12 \times 4$) for the density of states calculations. The electronic and structural optimization is conducted following the convergence criteria of 1×10^{-6} Ry, 1×10^{-5} Ry/Bohr, and 5×10^{-1} kbar for the energy, force and pressure respectively. These convergence criteria show good consistencies for both electronic and structural parameters of both systems. LDA and GGA-PBE functionals are also used for the structural, electronic, and elastic properties following same k-points arrangements and convergence criteria, with reduced kinetic energy cut-off. The elastic parameters of bulk (B) and young (E) modulus of α-Al_2O_3 is calculated based on Voigt-Reuss-Hill approximation as implemented in thermo_pw v.1.6.0. package by utilizing the optimized crystal structure from the initial calculation, and fixed the atomic positions.

RESULTS AND DISCUSSION

Optimized structures for both systems are described in Fig. 2 and its calculated values are summarized in Table 1. For comparison, we also include the calculated lattice parameter values from LDA and GGA-PBE functional [35,36]. For α-Al_2O_3 system, the calculated lattice parameter of a and c-values based on r++SCAN functional are 4.781 Å and 13.022 Å. These values are 0.52 % and 0.31 % higher compared to the experimental result [9]. Reported calculated values based on LDA functional are 0.98 % and 1.0 % smaller, while GGA-PBE functional lattice parameters (a and c) are overestimated by either 0.59 % and 0.66 % [35], or 1.03 % and 1.02 % [36]. The difference on the reported GGA-PBE

results could be very likely due to the different initial calculation's condition (kinetic energy cut-off, sampling k-points, convergence criteria, DFT-code, etc.). Similar situation is observed for α-Al_2S_3 system, where the difference between our calculated results and the experimental data are 0.67 % and 0.50 % higher for a and c-lattice parameter. The LDA functional underestimate the lattice parameter by 1.71 % and 1.27 %, while the GGA-PBE functional overestimate the lattice parameters by 1.88 % and 0.89 %. Looking into those results, the r++SCAN functional gives a better estimation on the lattice parameters for both α-Al_2O_3 and α-Al_2S_3 system, albeit with a slightly overestimated lattice parameter that is also previously reported on different systems [29]. The better accuracy on estimating the lattice parameter by this type of functional is due to its capability to describe the atomic-bonding interaction properly [21].

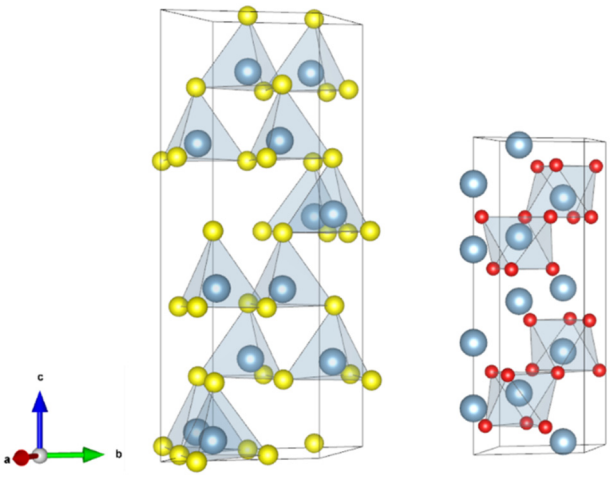

Figure 2. Optimized structure of **α**-Al_2S_3 and **α**-Al_2O_3. Red and yellow balls indicate S and O atom, while silver balls show the coordinate for Al atom. The drawings are produced by VESTA software [34]

Table 1. Optimized lattice parameter of α-Al_2O_3 and α-Al_2S_3

	LDA	GGA-PBE	r++SCAN	Experiment
		α-Al_2O_3		
a (Å)	4.709[a]	4.784[a] 4.805[b]	4.781	4.756[c]
c (Å)	12.846[a]	13.068[a] 13.116[b]	13.022	12.982[c]
V (Å)	246.740[a]	259.072[a] 262.252[b]	257.787	254.338[c]
		α-Al_2S_3		
a (Å)	6.330[d]	6.562[d]	6.473	6.438[e]
c (Å)	17.660[d]	18.054[d]	17.970	17.898[e]
V (Å)	612.808[d]	673.386[d]	652.080	640.206[e]

[a]Ref. 35 [b]Ref. 36 [c]Ref. 9 [d]This work [e]Ref. 6

We further analyze both system from density of states (DOS) and partial density of states (PDOS) calculations. It was known from previous studies that the calculated gap of a system depends on the functional. Our calculated data shows that the α-Al_2O_3 have an insulating gap of 10.3 eV. This value is actually larger compared to the optical gap (8.8 eV) and the value provided by SCAN functional (7.2 eV) with the same calculation's condition. Similar situation is also reported by Swathilakshmi *et al.,* where the r^{2}SCAN band gap gives larger value compared to SCAN functional for oxide system such as V_2O_5, CrO_3, MnO, and Fe_2O_3 [37]. Even by changing the exchange-part to the more accurate r^{4}SCAN functional, we also observed similar ~10 eV gap for α-Al_2O_3. The fact that similar trend (r++SCAN gives larger gap compared to SCAN) is observed on the oxide system, we believe that more detailed study needs to be addressed for this type of system in the future. Other possibilities that the 8.8 eV gap obtained from the experiment are considered to be an optical gap in which by definition is lower than the fundamental gap estimated by DFT calculation. Nevertheless, the DOS general characteristics for α-Al_2O_3 is the same with previous study based on GGA-PBE functional, with the valence states are dominated by oxygen and the conduction states mainly originated from aluminium as shown in Fig. 3(a). Looking into its orbital contribution on Fig. 3(c,d), we observe that the conduction states are originated from the hybridized states between s-p-d orbitals of Al-O. This is actually differs with what is shown from the previous GGA-PBE result, where only s and p-orbital that is observed [35], but consistent with the interpretation of experimental XANES data, where the distorted nature of the Al-O octahedral structure allowed such hybridization (s-p-d) to be exist [38].

Moving on to the α-Al_2S_3 system, the calculated insulating gap by using r++SCAN functional is 4.1 eV, which is very close to the experimental value of 4.2 eV. The DOS general characteristic for both conduction and the highest valence states is dominated by sulfur. This calculated value significantly improves the results obtained from the PBE (2.72 eV and ~3 eV) and LDA (2.51 eV) functionals [18]. As the gap value given by hybrid functional HSE06 is 4.95 eV [19], r++SCAN functional seems to improve the accuracy of HSE06. However, the experimental 4.2 eV gap is considered to be an optical instead of fundamental gap that is calculated from DFT technique. Thus, one can always argue that r++SCAN functional slightly underestimates the insulating gap of α-Al_2S_3. While the trend of r++SCAN functional calculated gap in respect to the reported hybrid functional seems to be differs for both α-Al_2O_3 and α-Al_2O_3 system (higher in α-Al_2O_3 and lower in α-Al_2O_3), note that the SCAN-type functional is a "parameter-free" calculation (additional parameter are set without any reference to the real systems) while hybrid functional depends on the adjusted mixing parameter (exact Hartree-Fock exchange) that differs on different systems and need to be adjusted accordingly. Therefore, whether r++SCAN functional gives a better electronic structure prediction compared to the reported hybrid functional is still an open question.

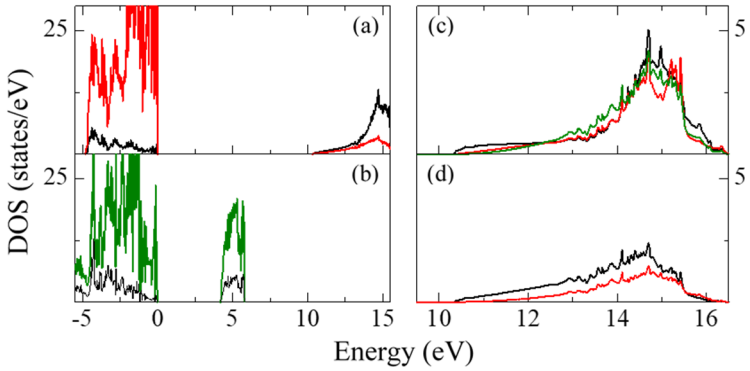

Figure 3. Density of states for (a) **α**-Al_2O_3 and (b) **α**-Al_2S_3. Black solid lines indicate Al electronic states, while blue and green lines indicate O and S electronic states. The highest valence state energy for each system is defined as 0 eV. (c) Orbital contribution of s (black), p (red), and d-orbitals (green) for Al atom (d). Orbital contribution of s (black) and p-orbitals (red) for O atom

Finally, we discuss about the calculated elastic parameters of α-Al_2O_3 and α-Al_2S_3 and compare to the previous study based on PBE functional and known experimental data. All calculated elastic parameters are summarized in Table 2. For α-Al_2O_3 system, r++SCAN functional overestimates the elastic constants of C_{11} by 3.01 %, C_{22} by 8.98 % and slightly underestimate the bulk (B) and young (E) modulus by 10.36 % and 6.21 % respectively when compared to experimental observation [39]. From the elastic parameter calculation of α-Al_2O_3, the calculated values given by r++SCAN are better compared to the results obtained by PBE functional [40], where the PBE functional significantly underestimates all elastic parameters (9.23 % for C_{11}, 9.58 % for C_{66}, 17.14 % for B, and 19.29 % for E). Furthermore, the experimental values of C_{11} and C_{66} are obtained at room temperature (~297 K) and tends to be reduced with an increasing temperature. Thus, by fitting the reported data with the 2nd order polynomial function, the fitted value at 0 K is 510 GPa and 171 GPa for C_{11} and C_{66} respectively, aligning more with our calculated r++SCAN results. To the best of author's knowledge, there is no experimental report on α-Al_2S_3 elastic parameter, however similar trend is observed where r++SCAN functional gives larger elastic parameters compared to the PBE functional.

Table 2. Calculated elastic parameters of α-Al_2O_3 and α-Al_2S_3

	C_{11} (GPa)	C_{66} (GPa)	B (GPa)	E (GPa)
		α-Al_2O_3		
r++SCAN	513	182	251	423
GGA-PBE[a]	452	151	232	364
Experiment[b]	498	167	280	451
		α-Al_2S_3		
r++SCAN	162	59	77	127
GGA-PBE[a]	150	55	71	116

[a]This work [b]Ref. 39

CONCLUSION

Structural, electronic, and elastic properties of α-Al_2O_3 and α-Al_2S_3 were studied using DFT technique by utilizing r++SCAN functional. Calculated lattice parameters show improvement over LDA and GGA-PBE functionals. Insulating gap of α-Al_2O_3 and α-Al_2S_3 are determined to be 10.3 eV and 4.1 eV. Compared to the known experimental values,

calculated values of α-Al_2O_3 is larger in contrast to the underestimated gap trend of semilocal functional. For α-Al_2S_3 system, the values are slightly underestimated and shows better accuracy compared to the past studies based on LDA, GGA, and hybrid functionals. Detailed description of α-Al_2O_3 electronic orbital in the conduction states shows hybridized s-p-d orbital confirming the interpretation of known XANES data. Calculated bulk and young modulus for α-Al_2O_3 are 251 and 423 GPa respectively, and relatively consistent with the known experimental data.

Acknowledgments

This study is supported by ITS grant No.941/PKS/ITS/2022 and No. 1724/PKS/ITS/2023. The computation in this work has been done using the facilities of MAHAMERU BRIN HPC, National Research and Innovation Agency of Indonesia (BRIN).

ORCID

Fahmia Astuti, https://orcid.org/0000-0003-1767-6202; **Muhammad Redo Ramadhan,** https://orcid.org/0000-0002-5115-5307

REFERENCES

[1] Y. He, B. Matthews, J. Wang, S. Li, X. Wang, and G. Wu, Journal of Materials Chemistry. A, Materials for Energy and Sustainability **6**, 735 (2018). https://doi.org/10.1039/C7TA09301B
[2] X. Zhang, L. Li, E. Fan, Q. Xue, Y. Bian, F. Wu, and R. Chen, Chemical Society Reviews, **47**, 7239 (2018). https://doi.org/10.1039/C8CS00297E
[3] D.-W. Han, S.-J. Lim, Y.-I. Kim, S.-H. Kang, Y.C. Lee, and Y.-M. Kang, Chemistry of Materials, **26**, 3644 (2014). https://doi.org/10.1021/cm500509q
[4] T.K. Mueller, G. Hautier, A. Jain, and G. Ceder, Chemistry of Materials **23**, 3854 (2011), https://doi.org/10.1021/cm200753g
[5] W. Chu, X. Zhang, J. Wang, S. Zhao, S. Liu, and H. Yu, Energy Storage Materials, **22**, 418 (2019). https://doi.org/10.1016/j.ensm.2019.01.025
[6] B. Krebs, A. Schiemann, and M. Läge, Zeitschrift Für Anorganische Und Allgemeine Chemie, **619**, 983 (1993). https://doi.org/10.1002/zaac.19936190604
[7] A. Eftekhari, Solid State Ionics, **167**, 237 (2004). https://doi.org/10.1016/j.ssi.2004.01.016
[8] W.-K. Kim, D. Han, W. Ryu, S. Lim, and H. Kwon, Electrochimica Acta, **71**, 17 (2012). https://doi.org/10.1016/j.electacta.2012.03.090
[9] M. Lucht, M. Lerche, H.-C. Wille, Yu.V. Shvyd'ko, H.D. Rüter, E. Gerdau, and P. Becker, Journal of Applied Crystallography, **36**, 1075 (2003). https://doi.org/10.1107/S0021889803011051
[10] R.H. French, Journal of the American Ceramic Society, **73**, 477 (1990). https://doi.org/10.1111/j.1151-2916.1990.tb06541.x
[11] R.H. Bube, *Photoconductivity of Solids*, (Wiley, 1960). pp. 172
[12] Y. Xu and W. Y. Ching, Physical Review B, **43**, 4461 (1991). https://doi.org/10.1103/physrevb.43.4461
[13] T.V. Perevalov, V.A. Gritsenko, and V.V. Kaichev, European Physical Journal-Applied Physics, **52**, 30501 (2010). https://doi.org/10.1051/epjap/2010159
[14] M. Bortz, and R.H. French, Applied Physics Letters, **55**, 1955 (1989). https://doi.org/10.1063/1.102335
[15] M.E. Innocenzi, R.T. Swimm, M. Bass, R.H. French, A. Villaverde, and M.R. Kokta, Journal of Applied Physics, **67**, 7542 (1990). https://doi.org/10.1063/1.345817.
[16] M. Choi, A. Janotti, and C.G. Van De Walle, Journal of Applied Physics, **113**, 044501 (2013). https://doi.org/10.1063/1.4784114
[17] J. Muscat, A. Wander, and N.M. Harrison, Chemical Physics Letters, **342**, 397 (2001)., https://doi.org/10.1016/S0009-2614(01)00616-9
[18] D. Zhang, X. Zhang, B. Wang, S. He, S. Liu, M. Tang, and H. Yu, Journal of Materials Chemistry, A, Materials for Energy and Sustainability, **9**, 8966 (2021). https://doi.org/10.1039/D1TA01422F
[19] S. Lysgaard, and J.M.G. Lastra, Journal of Physical Chemistry C, **125**, 16444 (2021). https://doi.org/10.1021/acs.jpcc.1c04484
[20] B. Ramogayana, D. Santos-Carballal, K.P. Maenetja, N.H. De Leeuw, and P.E. Ngoepe, ACS Omega, **6**, 29577 (2021) https://doi.org/10.1021/acsomega.1c03771
[21] J. Sun, A. Ruzsinszky, and J.P. Perdew, Physical Review Letters, **115**, 036402 (2015). https://doi.org/10.1103/physrevlett.115.036402
[22] C. Lane, J.W. Furness, I. Buda, Y. Zhang, R.S. Markiewicz, B. Barbiellini, J. Sun, and A. Bansil, Physical Review B, **98**, 125140 (2018). https://doi.org/10.1103/physrevb.98.125140
[23] M.R. Ramadhan, F. Astuti, J. Anavisha, I.M. Al-Hafiiz, W.R. Tiana, A. Oktaviana, M. Meireni, and D. Parwatiningtyas, Computational Condensed Matter, **32**, e00709 (2022). https://doi.org/10.1016/j.cocom.2022.e00709
[24] Y. Yao, and Y. Kanai, Journal of Chemical Physics, **146**, (2017). https://doi.org/10.1063/1.4984939
[25] J. Anavisha, A.F. Gunawan, D. Alfanny, W.R. Tiana, L. Yuliantini, J. Angel, D. Parwatiningtyas, and M.R. Ramadhan, AIP Conference Proceedings, **2708**, 020006 (2022). https://doi.org/10.1063/5.0122539
[26] H.-D. Saßnick, and C. Cocchi, Electronic Structure, **3**, 027001 (2021). https://doi.org/10.1088/2516-1075/abfb08
[27] A.P. Bartók, and J.R. Yates, Journal of Chemical Physics, **150**, 161101 (2019). https://doi.org/10.1063/1.5094646
[28] D. Mejía-RodríGuez, and S.B. Trickey, Physical Review B, **102**, 121109 (2020). https://doi.org/10.1103/PhysRevB.102.121109
[29] J.W. Furness, A.D. Kaplan, J. Ning, J.P. Perdew, and J. Sun, Journal of Chemical Physics, **156**, 034109 (2022). https://doi.org/10.1063/5.0073623
[30] R. Kingsbury, A. Gupta, C.J. Bartel, J.M. Munro, S. Dwaraknath, M. Horton, and K.A. Persson, Physical Review Materials, **6**, 013801 (2022). https://doi.org/10.1103/PhysRevMaterials.6.013801
[31] P. Giannozzi, S. Baroni, N. Bonini, M. Calandra, R. Car, C. Cavazzoni, D. Ceresoli, et al., Journal of Physics: Condensed Matter, **21**, 395502 (2009). https://doi.org/10.1088/0953-8984/21/39/395502
[32] P. Giannozzi, O. Andreussi, T. Brumme, O. Bunău, M. B. Nardelli, M. Calandra, R. Car, et al., Journal of Physics: Condensed Matter, **29**, 465901 (2017). https://doi.org/10.1088/1361-648x/aa8f79
[33] S. Lehtola, C. Steigemann, M.J.T. Oliveira, and M.A.L. Marques, SoftwareX, **7**, 1 (2018). https://doi.org/10.1016/j.softx.2017.11.002

[34] K. Momma, and F. Izumi, Journal of Applied Crystallography, **44**, 1272 (2011). https://doi.org/10.1107/S0021889811038970
[35] R.C.R. Santos, E. Longhinotti, V.N. Freire, R.B. Reimberg, and E.W.S. Caetano, Chemical Physics Letters, **637**, 172 (2015). https://doi.org/10.1016/j.cplett.2015.08.004
[36] A. Jain, G. Hautier, C. Moore, S.P. Ong, C.R. Fischer, T. Mueller, K.A. Persson, and G. Ceder, Computational Materials Science, **50**, 2295 (2011). https://doi.org/10.1016/j.commatsci.2011.02.023
[37] S. Swathilakshmi, R.K.V. Devi, and G.S. Gautam, (2023). https://arxiv.org/abs/2301.00535
[38] J.A. Van Bokhoven, T. Nabi, H. Sambé, D.E. Ramaker, and D.C. Koningsberger, Journal of Physics: Condensed Matter, **13**, 10247 (2001). https://doi.org/10.1088/0953-8984/13/45/311
[39] S.V. Sinogeikin, D.L. Lakshtanov, J.D. Nicholas, J.M. Jackson, and J.D. Bass, Journal of the European Ceramic Society, **25**, 1313 (2005). https://doi.org/10.1016/j.jeurceramsoc.2005.01.001
[40] M. De Jong, W. Chen, T. Angsten, A. Jain, R. Notestine, A. Gamst, M.H.F. Sluiter, et al., Scientific Data **2**, (2015), https://doi.org/10.1038/sdata.2015.9

РОЗРАХУНОК ЕЛЕКТРОННОЇ СТРУКТУРИ СИСТЕМИ α-Al_2X_3 (X=O,S) НА ОСНОВІ ФУНКЦІОНАЛУ R++SCAN

Мухаммад Р. Рамадхан[a], Салва А. Ханса[a], Коріана Зуліндра[a], Діан П. Хандаяні[a], Ніна А. Вардані[a], Фахмія Астуті[b]
[a] *Кафедра хімічної інженерії, факультет промислової інженерії, 55283 Слеман, Індонезія*
[b] *Кафедра фізики, Факультет науки та аналізу даних, Інститут технологій Сепулух Нопембер, 60111 Сурабая, Індонезія*

Через необхідність зменшення залежності від викопного палива кілька систем вважаються альтернативою та/або додатковою підтримкою для існуючого матеріалу батареї. У цьому звіті структурні та електронні властивості оксиду алюмінію (Al_2O_3) і сульфіду алюмінію (Al_2S_3) з гексагональною симетрією (α-фаза) досліджуються за допомогою техніки теорії функціоналу густини на основі функціоналу r++SCAN. Розрахований параметр решітки та ізоляційний зазор для обох систем добре узгоджуються з попередніми експериментальними дослідженнями та демонструють вищу точність порівняно з результатами досліджень апроксимації локальної щільності (LDA) та узагальненої градієнтної апроксимації (GGA). Розраховані значення ізоляційного зазору становлять 10,3 еВ і 4,1 еВ для α- Al_2O_3 і α- Al_2S_3 відповідно. Для системи α- Al_2O_3 ми спостерігали гібридизовану s-p-d-орбіталь Al-O у станах провідності, що узгоджується з інтерпретацією минулих даних поглинання рентгенівського випромінювання біля краю структури (XANES). Нарешті, об'ємний і молодий модуль для α- Al_2O_3 визначено як 251 ГПа і 423 ГПа, що дуже близько до відомих експериментальних значень 280 ГПа і 451 ГПа.

Ключові слова: *DFT; мета-GGA; r++SCAN; α-Al_2O_3, α-Al_2S_3*